Asymptotic accuracy of geoacoustic inversions

Michele Zanolin,[a] Ian Ingram, Aaron Thode, and Nicholas C. Makris
Massachusetts Institute of Technology, 77 Massachusetts Avenue, Cambridge, Massachusetts 02139

(Received 18 April 2003; revised 17 June 2004; accepted 9 July 2004)

Criteria necessary to accurately estimate a set of unknown geoacoustic parameters from remote acoustic measurements are developed in order to aid the design of geoacoustic experiments. The approach is to have estimation error fall within a specified design threshold by adjusting controllable quantities such as experimental sample size or signal-to-noise ratio (SNR). This is done by computing conditions on sample size and SNR necessary for any estimate to have a variance that (1) asymptotically attains the Cramer–Rao lower bound (CRLB) and (2) has a CRLB that falls within the specified design error threshold. Applications to narrow band deterministic signals received with additive noise by vertical and horizontal arrays in typical continental shelf waveguides are explored. For typical low-frequency scenarios, necessary SNRs and samples sizes can often approach prohibitively large values when a few or more important geoacoustic parameters are unknown, making it difficult to attain practical design thresholds for allowable estimation error. © *2004 Acoustical Society of America.* [DOI: 10.1121/1.1787526]

PACS numbers: 43.30.Pc [WLS] Pages: 2031–2042

I. INTRODUCTION

Geoacoustic parameters of the ocean floor strongly affect sound propagation and acoustic sensing in shallow water ocean waveguides where extensive bottom interaction occurs.[1–3] A significant amount of work has been done in recent years to develop methods for estimating geoacoustic parameters and to benchmark these methods against simulated noiseless data as for example in Refs. 2 and 4–10. Much less work, however, has been done to assess the performance of geoacoustic inversions in the presence of noise.[2,11–15]

Nonlinear inversions are often required to estimate geoacoustic parameters from measured acoustic field data. Since the measured data undergo random fluctuations due to additive noise, waveguide scintillation, or source randomness, this nonlinearity often leads to estimates that are biased and exceed the Cramer–Rao lower bound (CRLB) by orders of magnitude. In these situations, exact expressions for the bias and the variance are often difficult or impractical to derive analytically.

Knowing both the CRLB and how to attain it is useful for a number of practical reasons. The mean-square error of any unbiased estimate of a deterministic parameter vector from random data cannot be less than the CRLB, which exists given mild regularity conditions on the probability density of the data.[16] This is true *regardless of the method of estimation*, and, for example, regardless of whether or not there are significant ambiguities, sometimes referred to as *sidelobes* in the estimation problem.

Parameter estimates only have practical value if their errors fall within the design thresholds specified for the given experiment. In the inversion of geoacoustic parameters, for example, design errors are often set by the needs of those who run propagation and scattering models to evaluate sonar system performance. If the CRLB for a particular experiment is always greater than the specified design error threshold, the experiment will never be able to achieve its goals and will necessarily fail. So the CRLB on its own is extremely useful as a tool in aiding experimental design in these situations. If the CRLB is less than or equal to the allowable design error, on the other hand, the practicality of the experimental design is still questionable until it is established that the parameter estimates derived from this experiment actually attain the CRLB.

Since necessary conditions for an estimate to attain the CRLB are now available and depend on controllable variables of an experiment such as signal-to-noise ratio (SNR) or sample size,[17] and the CRLB is also a function of these controllable variables, conditions are then also available to attain any specified design error. This can be done by proper adjustment of the controllable variables.

Along these lines, we follow the general estimation theory approach introduced in Ref. 17 and use it to derive conditions to accurately estimate a set of unknown geoacoustic parameters from remote acoustic field measurements. We do this by computing necessary SNRs and sample sizes for the estimates to become asymptotically unbiased, for their mean-square errors to attain the CRLB, and then for the CRLB to fall within any specified design criteria.

We note that the approach of Ref. 17 is a general consequence of estimation theory and so can be and has already been applied to obtain optimality conditions and to extract new physical insights in a number of widely divergent and physically unrelated estimation problems. These include time-delay and Doppler shift estimation,[17] source localization in an ocean waveguide,[18] and pattern recognition in 2-D images,[19] where an *optimal estimate* in this context is defined as being unbiased and having minimum variance following standard practice.[20] A basic advantage of this approach is that it is typically straightforward to implement and provides analytical insight into the mechanics of asymptotic optimality and consequently attainable accuracy for the given estima-

[a]Electronic mail: zanolin@mit.edu

tion problem. Brute force numerical calculation of estimator moments does not easily offer such insight, but is the only alternative currently available.

Our present analysis focuses on aiding experimental design by determining necessary SNRs and sample sizes to attain practical accuracies in estimating geoacoustic parameters of the seafloor from standard ocean-acoustic inverse experiments. We consider narrow-band deterministic signals received with additive ambient noise by both vertical and horizontal arrays in continental shelf waveguides. Given the large number of unknown environmental parameters in such problems, it is common practice to invert for tens or more parameters simultaneously.[1,21–23] Various combinations of geoacoustic parameters for simultaneous inversion are considered and criteria necessary for accurate inversions are presented. The conditions are found to become significantly more stringent, sometimes to the point of being prohibitive, as the number of unknown parameters to which the measured field is sensitive increases.

In Sec. II, conditions necessary for asymptotic optimality are summarized in a more explicit form than has previously appeared, and a far more condensed and efficient form of the asymptotic variance is also provided. An explicit explanation of how these necessary conditions may be used to achieve design specifications for error thresholds in a given experiment also appears in Sec. II. Analysis of illustrative problems in geoacoustic inversion appear in Sec. III. Since the data are modeled as deterministic signals measured with random ambient noise, we have not investigated the effects of model mismatch or uncertainty in sensor location, both of which may also lead to significant errors. These effects, however, will only make the necessary conditions more stringent.

II. NECESSARY CONDITIONS FOR ASYMPTOTICALLY OPTIMAL ESTIMATION AND FOR ATTAINING SPECIFIED ERROR DESIGN THRESHOLDS

Consider a set of n independent and identically distributed experimental data vectors $\mathbf{X}_i$ of dimension N obeying the probability density $p(\mathbf{X};\boldsymbol{\theta})$, where $\mathbf{X}=[\mathbf{X}_1^T,\ldots,\mathbf{X}_n^T]^T$ and $\boldsymbol{\theta}$ is an m-dimensional parameter vector. The MLE $\hat{\boldsymbol{\theta}}$ of $\boldsymbol{\theta}$ maximizes the log-likelihood function $l(\mathbf{X};\boldsymbol{\theta})=\ln(p(\mathbf{X};\boldsymbol{\theta}))$ with respect to the components of $\boldsymbol{\theta}$. If the rth component of $\boldsymbol{\theta}$ is denoted by θ^r, the first log-likelihood derivative with respect to θ^r is then defined as $l_r=\partial l(\boldsymbol{\theta})/\partial\theta^r$. The elements of the expected information matrix, known as the Fisher matrix, are then given by $i_{ab}=E[l_a l_b]$, and the elements of its inverse by $i^{ab}=[\mathbf{i}^{-1}]_{ab}$, where $\mathbf{i}^{-1}$ is also known as the CRLB.

The moments of $\hat{\theta}^r$ for $r=1,...,m$ can be expressed as a series in inverse powers of the sample size n,[17,18] provided that the required derivatives of the likelihood function exist.[24] The variance can then be expressed as

$$var(\theta^r)=\frac{var_1(\theta^r)}{n}+\frac{var_2(\theta^r)}{n^2}+O\left(\frac{1}{n^3}\right), \tag{1}$$

where $O(1/n^3)$ represents integer powers higher than $1/n^2$ and $var_1(\theta^r)$ and $var_2(\theta^r)$ depend only on a single sample probability distribution. The first term on the right-hand side is the CRLB, which is the minimum variance for an unbiased estimate and also the asymptotic value of the variance in the limit as the sample size n and SNR approach infinity.

The sample size necessary for the MLE variance to asymptotically attain the CRLB is found by requiring the second-order variance to be negligible compared to the first

$$\frac{|var_2(\theta^r)/n^2|}{var_1(\theta^r)/n}\ll 1, \tag{2}$$

which implies

$$n\gg\frac{|var_2(\theta^r)|}{var_1(\theta^r)}. \tag{3}$$

Only for sample sizes satisfying this condition is it possible for the variance to be in the asymptotic regime where it continuously attains the CRLB. This follows from the fact that each term in the expansion is proportional to a unique power in $1/n$.

In a similar manner, a necessary sample size for the inversion to be asymptotically unbiased is found by requiring that the first-order bias is negligible compared to the true value of the parameter:

$$n\gg\frac{|b_1(\theta^r)|}{|\theta^r|}. \tag{4}$$

The conditions (3) and (4) provide insight into the performance of any estimate in the limit of large sample size or SNR. In fact, in this regime any estimate that satisfies these conditions must be the MLE.[20]

As noted in the Introduction, parameter estimates only have practical value if their errors fall within the design threshold specified for the given experiment. In order to attain a specified design error threshold by the present approach, the sample size n must be large enough that (I) optimality conditions (3) and (4) are satisfied and (II) the CRLB falls within the required design error threshold.

A. Statistical model for the acoustic data

We consider the field generated by a deterministic narrow band source that is received by an array of hydrophones with additive stationary ambient noise. One vector sample in the frequency domain of the measured field can be obtained from the Fourier transform of a time window of the acoustic measurements. Statistical independence of the samples requires them to have a sample spacing that is at least the coherence time of the total received field.[25] Explicitly, the jth spectral data sample $\tilde{\mathbf{X}}_j(\omega;\boldsymbol{\theta})$ for $j=1,...,n$ is given by

$$\tilde{\mathbf{X}}_j(\omega;\boldsymbol{\theta})=A(\omega)\tilde{\mathbf{g}}(\omega)+\tilde{\boldsymbol{\eta}}_j(\omega), \tag{5}$$

where $A(\omega)$ is the Fourier transform of the source amplitude, $\tilde{\mathbf{g}}(\omega)=[\tilde{g}_1(\omega;\boldsymbol{\theta}),\ldots,\tilde{g}_N(\omega;\boldsymbol{\theta})]$ is the vector of Green's functions in the frequency domain connecting the source location to the N hydrophone locations on the array, and $\tilde{\boldsymbol{\eta}}_j(\omega)=[\tilde{\eta}_{j1}(\omega),\ldots,\tilde{\eta}_{jN}(\omega)]$ is the noise spectral sample which is given by a Fourier transform of a finite time window of the noise.

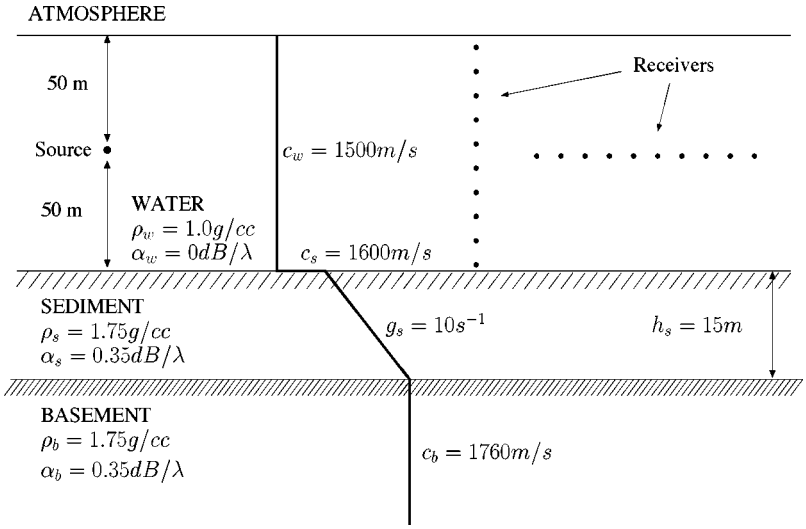

FIG. 1. Waveguide model and experimental setup. An isovelocity water column overlies a two-layer bottom: a 15-m-thick fluid sediment layer with a sound speed linearly increasing with depth stands above a basement with constant sound speed and density. A narrow band point source is located at the center of the wave guide and receiving arrays. A ten-element vertical array and horizontal arrays with 10 and 100 elements are considered. The spacing between the elements is 7.5 m and the arrays are centered in the water column.

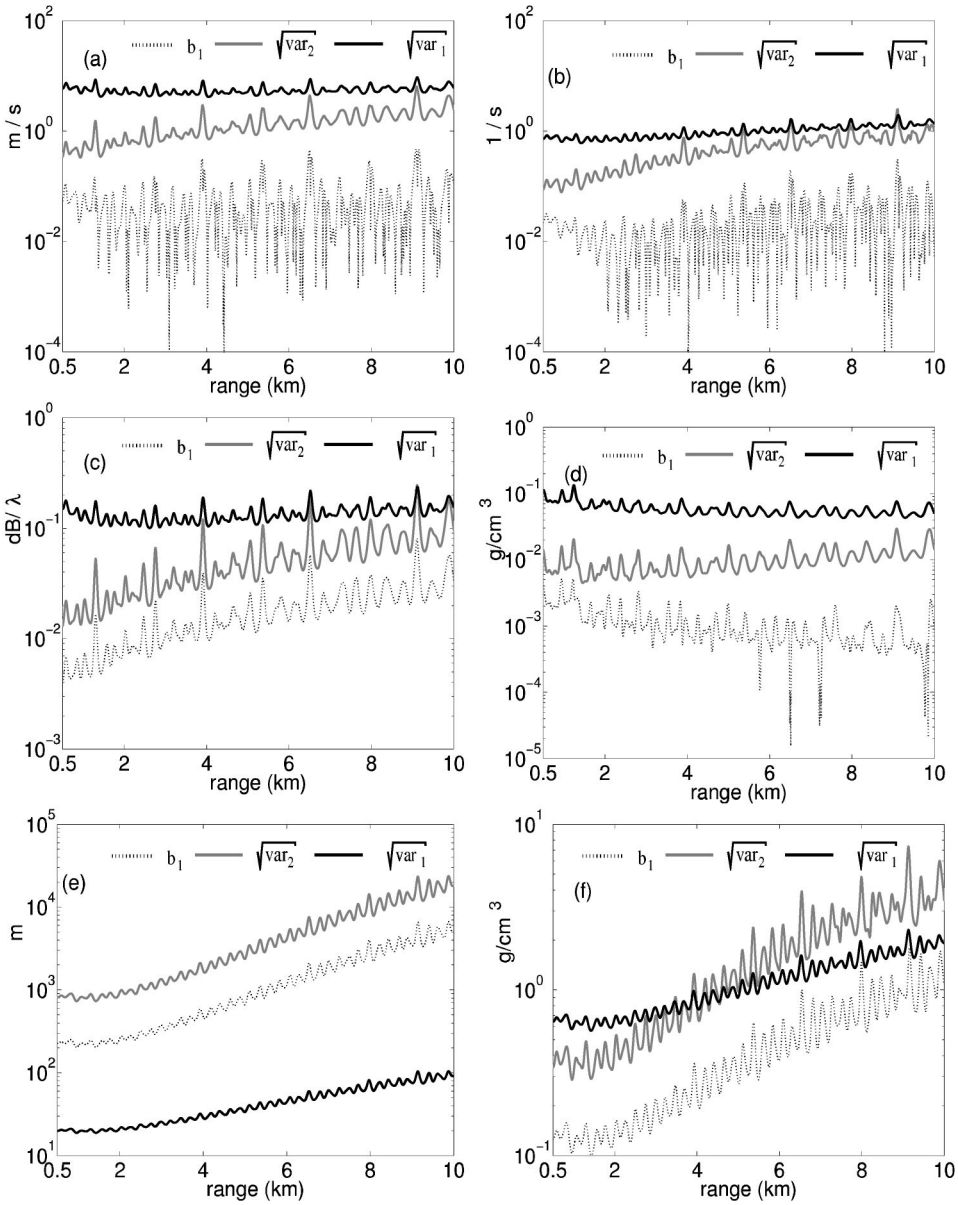

FIG. 2. $\sqrt{var_1}$ (black), $\sqrt{|var_2|}$ (gray), and b_1 (dotted) for single parameter estimates of c_s, g_s, α_s, ρ_s, h_s, and ρ_b are presented for $n=1$ as a function of range between 0.5 and 10 km for a 100-Hz source and ten-element vertical array centered at mid-depth in the watercolumn.

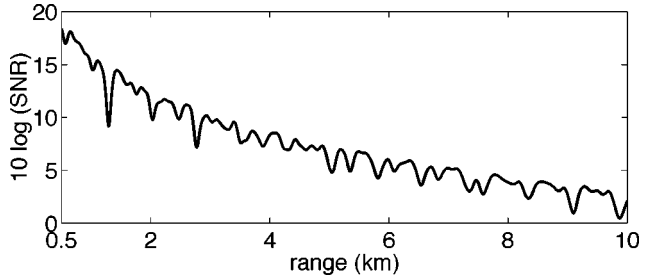

FIG. 3. SNR as functions of range between 0.5 and 10 km. Same experimental setup as Fig. 2.

The noise spectrum is well described by a circular complex Gaussian random variable (CCGR),[25,26] so that the probability density for the real measured data $\mathbf{X}_j$ with $j=1,...,n$ becomes

$$p(\mathbf{X},\boldsymbol{\theta})=(2\pi)^{-nN/2}|\mathbf{C}|^{-n/2} \times\exp\left\{-\frac{1}{2}\sum_{j=1}^{n}(\mathbf{X}_j-\boldsymbol{\mu}(\boldsymbol{\theta}))^T\mathbf{C}^{-1}(\mathbf{X}_j-\boldsymbol{\mu}(\boldsymbol{\theta}))\right\}, \tag{6}$$

where $\mathbf{X}_j$ and $\boldsymbol{\mu}(\boldsymbol{\theta})$ are specified by

$$\mathbf{X}_j=\begin{bmatrix}\mathrm{Re}(\tilde{\mathbf{X}}_j(\omega;\boldsymbol{\theta}))\\ \mathrm{Im}(\tilde{\mathbf{X}}_j(\omega;\boldsymbol{\theta}))\end{bmatrix},\quad \boldsymbol{\mu}(\boldsymbol{\theta})=\begin{bmatrix}\mathrm{Re}(A(\omega)\tilde{\mathbf{g}}(\omega))\\ \mathrm{Im}(A(\omega)\tilde{\mathbf{g}}(\omega))\end{bmatrix}, \tag{7}$$

with Re(.) and Im(.) indicating the real and imaginary parts. The real covariance matrix

$$\mathbf{C}=\frac{1}{2}\begin{pmatrix}\mathrm{Re}(\tilde{\mathbf{C}}) & -\mathrm{Im}(\tilde{\mathbf{C}})\\ \mathrm{Im}(\tilde{\mathbf{C}}) & \mathrm{Re}(\tilde{\mathbf{C}})\end{pmatrix} \tag{8}$$

is specified by the spectral complex covariance matrix of the noise across the array $\tilde{\mathbf{C}}$ whose elements are given by $\tilde{\mathbf{C}}_{ln}=E[\eta_{jl}(\omega)\eta_{jn}^*(\omega)]=\sigma^2\delta_{ln}$, with δ_{ln} equal to 1 for $l=n$ and 0 for $l\neq n$. Note that the expectation eliminates the dependence on the sample index j. Here we assume spatially uncorrelated noise for both the horizontal and vertical apertures based on our experience with experimental data in shallow water environments. An alternative would be to use theoretical predictions based on uniformly distributed surface noise sources such as in Ref. 27.

In the present formulation, while the measured field contains parameter information, the sufficient statistic for optimal estimation in a measurement is not the measured field or its ensemble average from measured data but the entire argument of the exponential, known as the Mahalobinos distance.[28] This preserves all the relevant intersensor phase information as the ensemble average of a positive semidefinite quantity.

For this statistical model, the expressions given in Ref. 17 for the numerators of the first-order bias and the first two orders of the variance can be expressed in the much more compact form

$$b_1(\theta^r)=-\tfrac{1}{2}i^{ra}i^{bc}\boldsymbol{\gamma}_{ac}^T\boldsymbol{\gamma}_b, \tag{9}$$

$$var_1(\theta^i)=-i^{ii}, \tag{10}$$

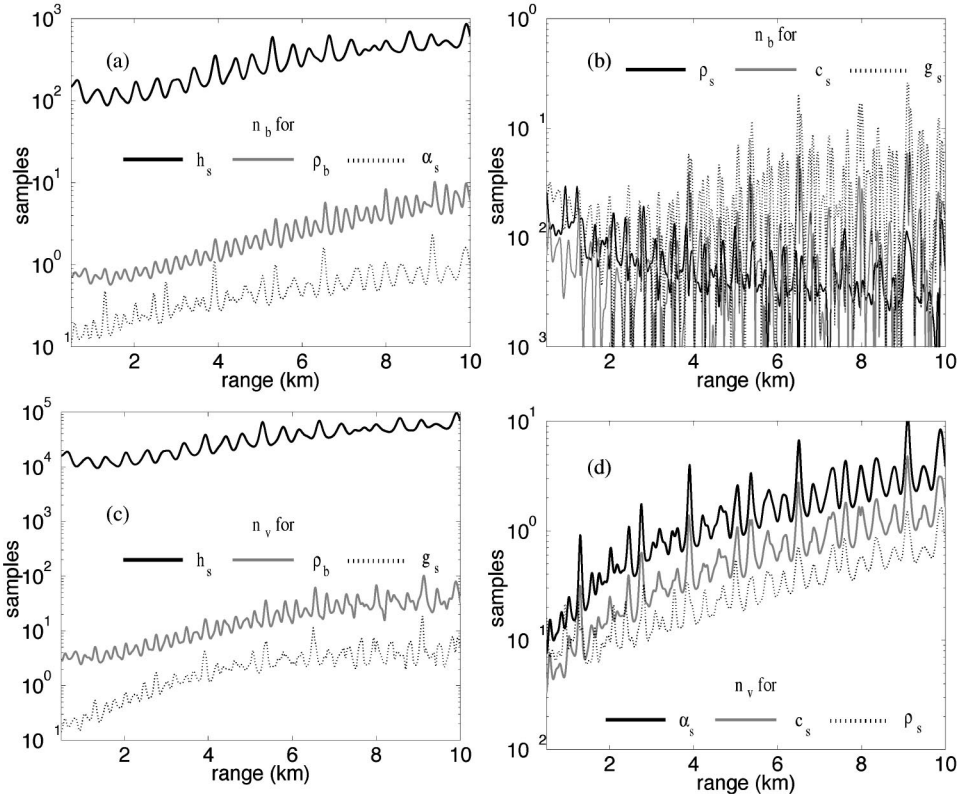

FIG. 4. n_b and n_v as functions of range between 0.5 and 10 km for single parameter. (a) n_b for h_s (black), ρ_b (gray), and α_s (dotted). (b) n_b for ρ_s (black), c_s (gray), and g_s (dotted). (c) n_v for h_s (black), ρ_b (gray), and ρ_b (dotted). (d) n_v for ρ_s (black), c_s (gray), and g_s (dotted). Same experimental setup as Fig. 2.

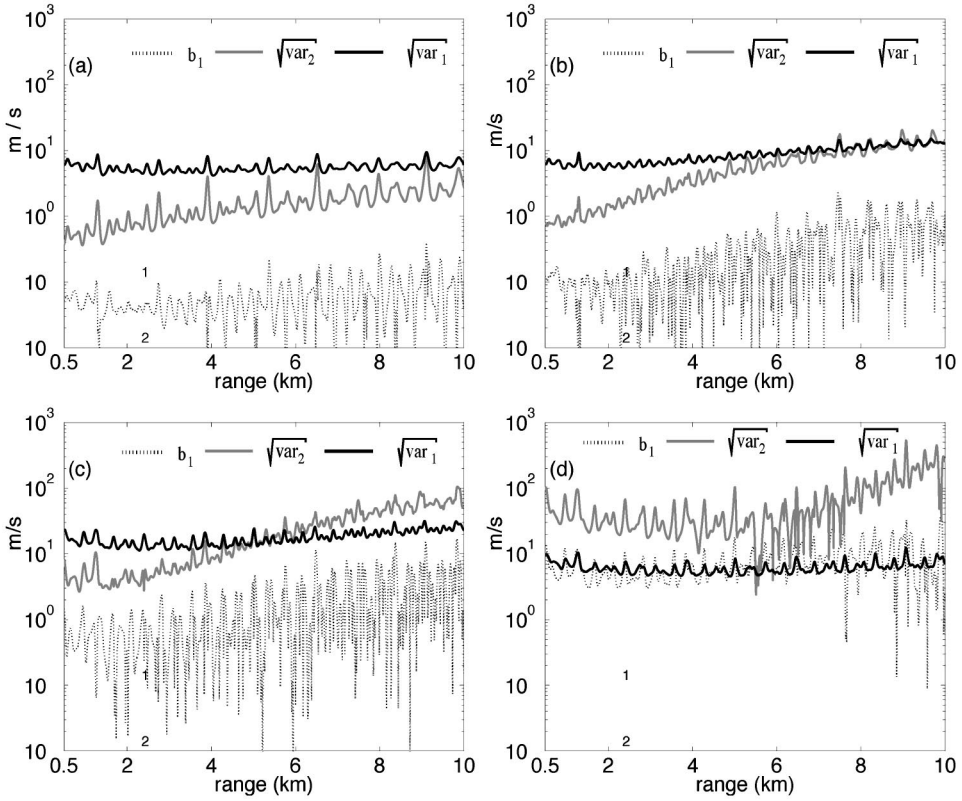

FIG. 5. $\sqrt{var_1}$ (black), $\sqrt{|var_2|}$ (gray), and b_1 (dotted) are shown as a function of range for $n=1$ between 0.5 and 10 km in inversions for c_s with one other unknown parameter. The unknown is successively (a) α_s, (b) ρ_s, (c) g_s, and (d) h_s. Same experimental setup as Fig. 2.

$$var_2(\theta^i) = i^{im} i^{in} i^{pq} \Bigg(\boldsymbol{\gamma}_{nq}^T \boldsymbol{\gamma}_{pm} - \boldsymbol{\gamma}_{mn}^T \boldsymbol{\gamma}_{pq} - \boldsymbol{\gamma}_{mpq}^T \boldsymbol{\gamma}_n + i^{zt} \Bigg(\frac{\boldsymbol{\gamma}_n^T \boldsymbol{\gamma}_{tq}}{2} \boldsymbol{\gamma}_m^T \boldsymbol{\gamma}_{zp} + (2\boldsymbol{\gamma}_{qt}^T \boldsymbol{\gamma}_n - \boldsymbol{\gamma}_{qn}^T \boldsymbol{\gamma}_t) \boldsymbol{\gamma}_{pm}^T \boldsymbol{\gamma}_z + (\boldsymbol{\gamma}_{mn}^T \boldsymbol{\gamma}_p + \boldsymbol{\gamma}_{mp}^T \boldsymbol{\gamma}_n) \boldsymbol{\gamma}_{zt}^T \boldsymbol{\gamma}_q \Bigg) \Bigg), \tag{11}$$

where $\boldsymbol{\gamma}_{c\cdots d} = [A(\omega)/\sigma]\mathbf{g}_{c\cdots d}$ and the subscripts $c\cdots d$ indicate that derivatives of the Green's function with respect to the parameters $\theta_c \cdots \theta_d$ have been taken. The Einstein summation convention is used so that if an index occurs twice in a term, once in the subscript and once in the superscript, summation over the index is implied.

The SNR for a single sample collected across the array

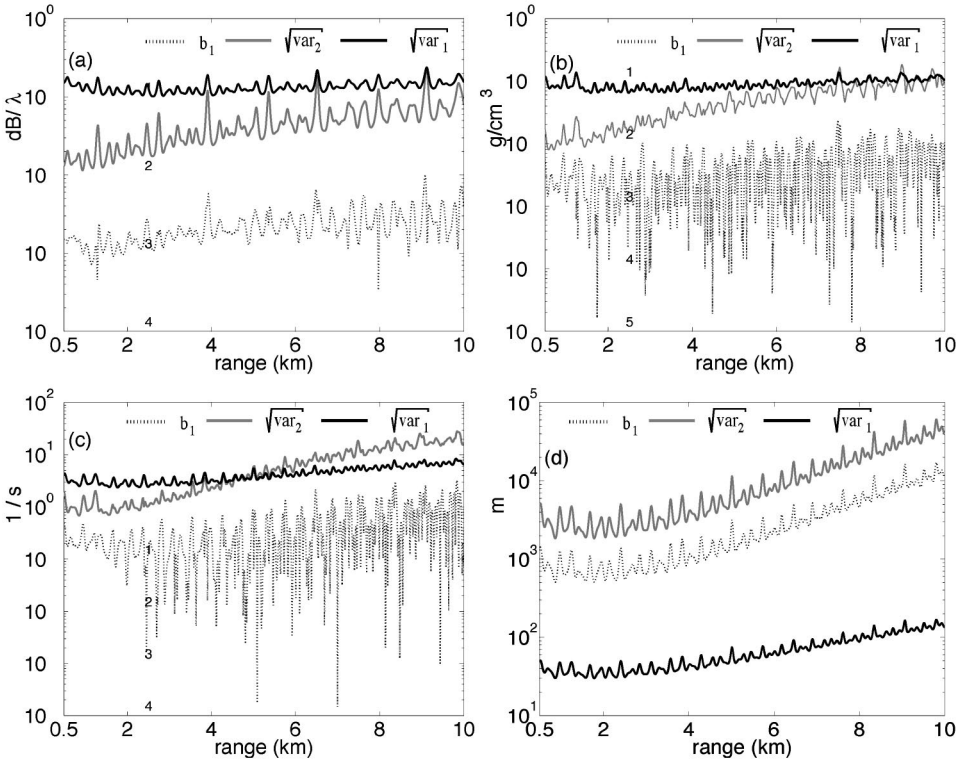

FIG. 6. $\sqrt{var_1}$ (black), $\sqrt{|var_2|}$ (gray), and b_1 (dotted) are shown as a function of range for $n=1$ between 0.5 and 10 km for successive two-parameter estimates of (a) α_s, (b) ρ_s, (c) g_s, and (d) h_s with c_s. Same experimental setup as Fig. 2.

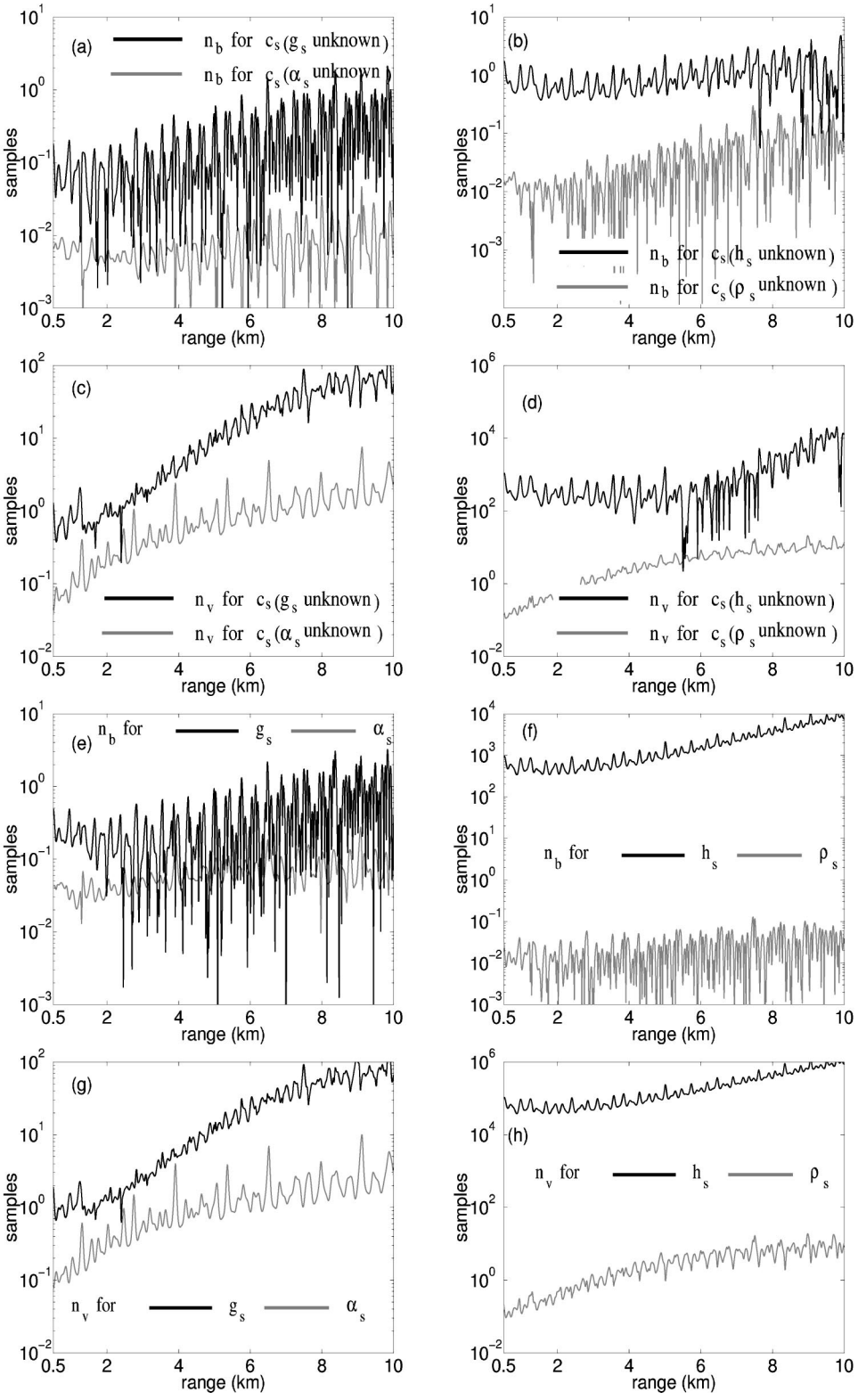

FIG. 7. For the estimation of c_s when a second parameter is unknown, n_b is presented when (a) α_s (gray) and g_s (black) are unknown (b) ρ_s (gray) and h_s (black) are unknown and n_v is presented when (c) α_s (gray) and g_s (black) are unknown and (d) ρ_s (gray) and h_s (black) are unknown. For the estimation of a sediment parameter when a c_s is unknown, n_b is presented for (e) α_s (gray) and g_s (black) and (f) ρ_s (gray) and h_s (black), and n_v is presented for (g) α_s (gray) and g_s (black) and (h) ρ_s (gray) and h_s (black).

has been defined as the ratio $\mathrm{SNR}=\boldsymbol{\mu}(\omega;\boldsymbol{\theta})\boldsymbol{\mu}(\omega;\boldsymbol{\theta})^*/\mathrm{tr}(\mathbf{C})=|\mathrm{A}(\omega)|^2\mathbf{g}(\omega;\boldsymbol{\theta})\mathbf{g}(\omega;\boldsymbol{\theta})^*/N\sigma^2$. In most geoacoustic inversion experiments performed in shallow water the SNR varies between 10 and 20 dB,[1,29,30] sometimes reaching values between 30 and 40 dB.[31] In the examples presented in this paper the SNR is set to 15 dB at a range of 1 km from the source, or, equivalently, the variance of the noise is fixed by

$$\sigma^2=\frac{1}{N}\left.\frac{|A(\omega)|^2\mathbf{g}(\omega;\boldsymbol{\theta})\mathbf{g}(\omega;\boldsymbol{\theta})^*}{10^{1.5}}\right|_{\text{range}=1\ \text{km}}. \tag{12}$$

III. ILLUSTRATIVE EXAMPLES

The conditions necessary to obtain an optimal parameter estimate in a given experimental scenario depend on a num-

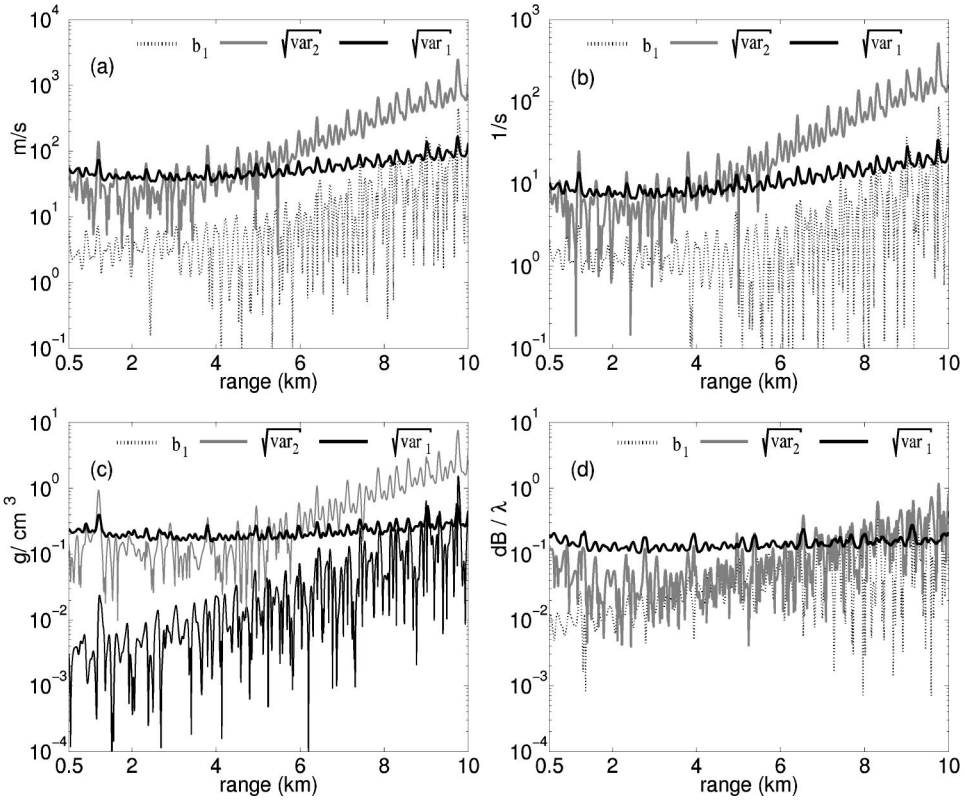

FIG. 8. Simultaneous four-parameter estimation of c_s, g_s, ρ_s, and α_s where $\sqrt{var_1}$ (black), $\sqrt{|var_2|}$ (gray), and b_1 (dotted) are presented for (a) c_s, (b) g_s, (c) ρ_s, and (d) α_s for $n=1$ as a function of range between 0.5 and 10 km. Same experimental setup as Fig. 2.

ber of variables, including the parameters involved in the inversion, the number of parameters simultaneously estimated, the frequency of the source, the range of the receivers, and the SNR. In order to isolate and illustrate these contributions, a number of simulations are performed in a waveguide representative of the continental shelf where a sediment layer overlays a bottom half-space, as shown in Fig. 1 using a modal formulation for the field as in Ref. 18. The numerical field derivatives approach used was benchmarked analytically in a Pekeris waveguide.[32] Field derivatives were also checked with three independent propagation codes including OASIS, SNAP, and a modified version of

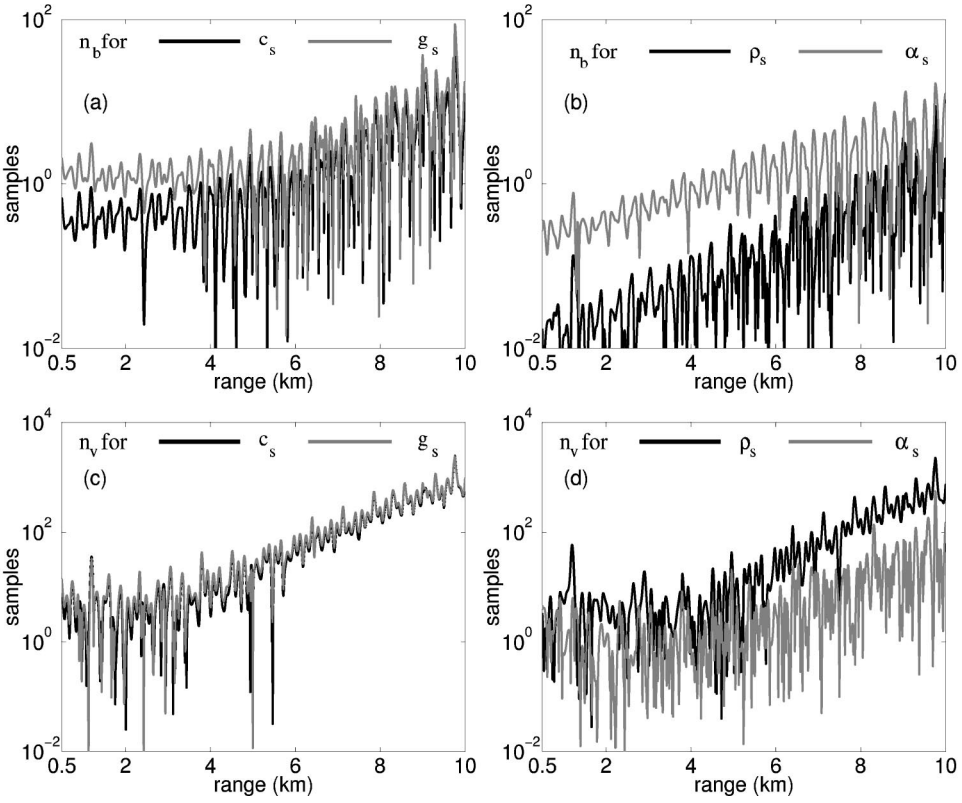

FIG. 9. Source frequency is 100 Hz. Necessary sample sizes for the simultaneous four-parameter estimation of c_s, g_s, ρ_s, and α_s: (a) n_b for c_s (black) and g_s (gray), (b) n_b for ρ_s (black) and α_s (gray), (c) n_v for c_s (black) and g_s (gray), and (d) n_v for ρ_s (black) and α_s (gray). Same experimental setup as Fig. 2.

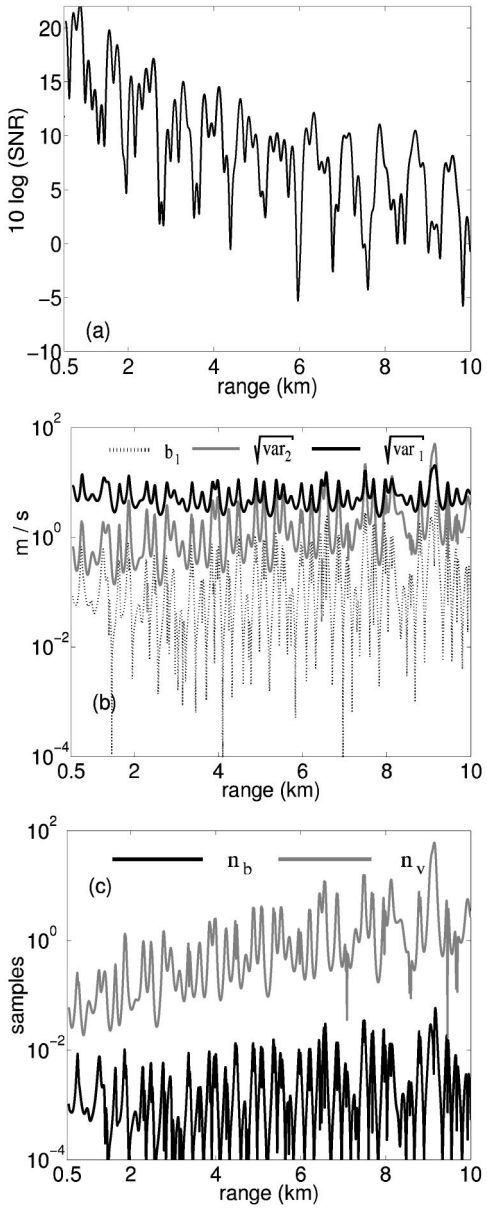

FIG. 10. Single parameter inversion of c_s using a ten-element horizontal array with 7.5-m spacing. The array is located at 50-m depth with 100-Hz source frequency. Shown for $n=1$ as a function of range between 0.5 and 10 km are (a) SNR, (b) $\sqrt{var_1}$ (black), $\sqrt{|var_2|}$ (gray), and b_1 (dotted), and (c) n_b (black) and n_v (gray).

KRAKEN. The sound speed profile in the sediment can be specified in terms of c_s and g_s as $c(z)=c_s+g_s(z-H)$, where the z axis originates at the water–atmosphere interface and is directed vertically downward.

To represent a typical experiment, in Secs. III A and III B a ten-element vertical array is centered in a water column of depth $H=100$ m with 7.5-m spacing between each element so that the shallowest element is at 16.25-m depth. The source is placed at 50-m depth. In this paper a 100-Hz deterministic monopole source is employed. Inversions performed with horizontal arrays are presented in Sec. III C to investigate the effect of array length and orientation on inversion performance.

The necessary sample sizes for the variance to attain the CRLB are computed by conservatively requiring in condition (3) that the second-order variance is ten times smaller than the CRLB for all parameters,

$$n \geqslant n_v = 10\frac{|var_2(\theta^r)|}{var_1(\theta^r)}. \tag{13}$$

Similarly, the necessary sample sizes for the inversions to be unbiased are computed by requiring in condition (4) that the first-order bias be ten times smaller than the true value of the parameter, or $n>n_b=10|b_1(\theta_j)|/|\theta_j|$ except for sound speeds where $n>n_b=200|b_1(\theta_j)|/|\theta_j|$ is used instead since these biases strongly affect the acoustic field. The conditions for an inversion to be optimal are then given by $n>n_b$ and $n>n_v$. If the computed values of n_v and n_b are less than unity, then only one sample is required and the figures can be used to determine how far the SNR can be lowered without sacrificing single-sample optimality. We especially note scenarios where n_b and n_v are large but the corresponding CRLB is small and vice-versa.

It should be noted that the illustrative examples can be used to determine SNR outside of the ranges explicitly shown due to the equivalence of n and SNR in the asymptotic expansions. For example, this means that the conditions (3) and (4) can be reformulated in terms of SNR, and that n_v and n_b are proportional to 1/SNR.

A. Single-parameter inversions

Here we investigate the requirements for estimation errors to attain specified design thresholds for single-parameter inversions. To do this we compute the sample sizes necessary for inversion optimality as well as the magnitude of the CRLB for a single sample. It is important to note that the former optimality condition need not be related to the parameter sensitivity expressed by the single-sample CRLB. This is because the optimality conditions involve higher order parameter derivatives than the CRLB.

The biases, variances, and necessary sample sizes n_v and n_b are computed as a function of source-receiver range for all eight single-parameter estimates allowable in the model. For our purposes only six of these need to be presented in Figs. 2 and 4. These are the thickness of the sediment layer h_s, the compressional wave speed at the top of the sediment layer c_s, the gradient of the compressional wave speed g_s, the attenuation in the sediment α_s, the sediment density ρ_s, and the basement density ρ_b.

The decreasing trend in inversion accuracy with range for all parameters is mostly due to the decrease in SNR shown in Fig. 3 from both spreading and attenuation loss. Stripping of higher order modes with range also plays a role in the decreased accuracy. Estimates of c_s, ρ_s, α_s, and g_s require smaller sample size to be optimal than the basement density ρ_b, and significantly smaller sample size than the thickness of the sediment layer h_s which has particularly stringent optimality conditions. Hundreds of samples are necessary for the h_s estimate to be unbiased even at relatively close ranges and thousands of samples are necessary for the variance to attain the CRLB indicating that the sediment layer thickness h_s has a highly nonlinear relationship with the acoustic measurements.

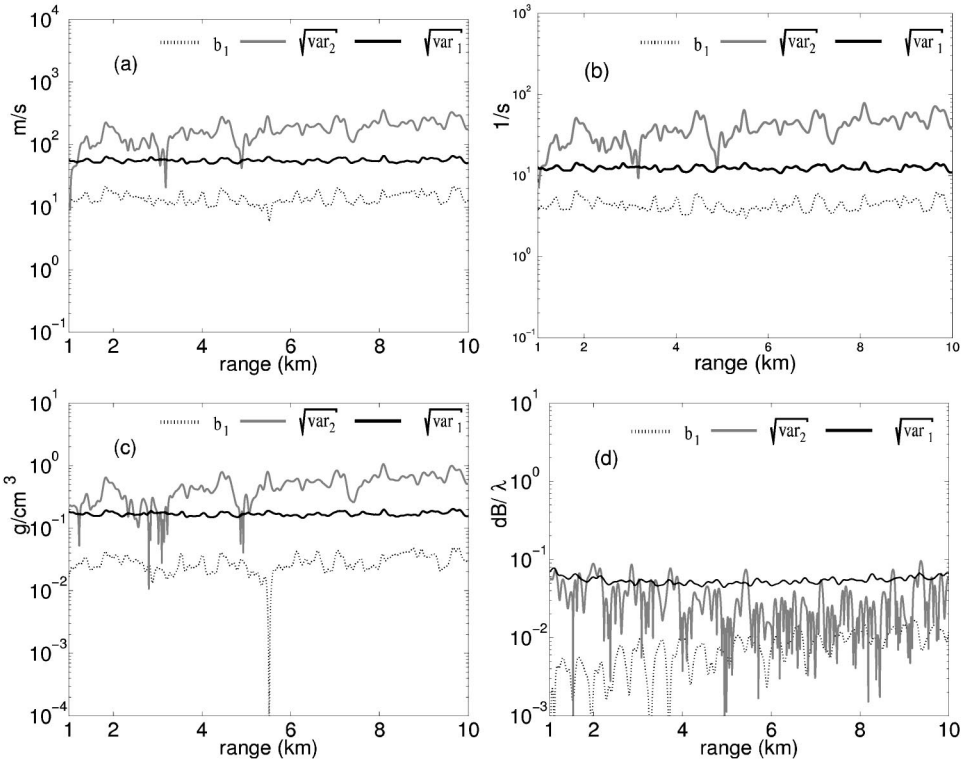

FIG. 11. Simultaneous four-parameter estimation of c_s, g_s, ρ_s, and α_s using a 100-element horizontal array with 7.5-m spacing. The array is located at 50-m depth and the source frequency is 100 Hz. $\sqrt{var1}$ (black), $\sqrt{|var_2|}$ (gray), and b_1 (dotted) are shown for $n=1$ as a function of range between 1 and 10 km for (a) c_s, (b) g_s, (c) ρ_s, and (d) α_s.

We note that while ρ_s and α_s have similar optimality conditions as c_s, the ratio of the square-root of the single-sample CRLB, which is inversly related to the sensitivity of the measurement to the parameter, to the true parameter value is on the order of at least 0.1 for ρ_s and α_s but is less than 0.01 for c_s. This highlights why the *two requirements* explicitly stated in Sec. II are necessary for a parameter estimate to attain a specified error threshold and knowledge of the CRLB alone is not enough.

The inversion of h_s, ρ_b, and the other basement parameters not explicitly presented here are significantly more difficult than the other sediment parameters because they require either prohibitlvely large sample sizes to attain optimality or because the square root of their single-sample CRLBs are large compared to the true parameter value. Sound in the water column is apparently less sensitive to basement parameters due to attenuation in the sediment for the given sediment thickness and acoustic frequency. Similar observations about this lack of sensitivity have been noted in Ref. 20 solely through CRLB analysis.

At lower frequency, penetration into the basement may be more substantial, but there may also be fewer modes. This could lead to difficulties in unambiguously inverting large parameter sets. The modal structure of the acoustic field, for example, imposes limitations on the number of bottom parameters of the given model that can be unambiguously determined with a single frequency source. To illustrate the situation, consider receivers in the water column of a Pekeris waveguide. Each mode is then described by four parameters, the real and imaginary components of the vertical wave number and of the mode's equivalent plane wave amplitude since the up- and downgoing plane wave amplitudes are the negative of each other in this case. This means that the effect of bottom properties on the acoustic field can only be expressed through $4M$ parameters, where M is the number of modes, making $4M$ an upper limit on the number of bottom parameters that can be unambiguously estimated regardless of the number of receivers in the water column. Such limitations can be potentially overcome by increasing the bandwidth.

B. Multiparameter inversions

Simulations presented in this section show that estimation performance worsens as the number of parameters simultaneously inverted increases. To see this, the quantities b_1, var_1, var_2, n_b, and n_v are plotted as a function of source–receiver range for the simultaneous estimation of two parameters, namely c_s together successively with α_s, ρ_s, g_s, and then h_s in Figs. 5–7. Each pairing affects the estimation of c_s in different ways as can be seen in Fig. 5. In fact, estimation of c_s is effectively uncoupled from that of α_s because the two-parameter estimates yield results nearly identical to those of the corresponding single parameter estimates. This can be seen by comparing the moments in Figs. 5(a) and 6(a) with the corresponding ones in Fig. 2(a), and the necessary sample sizes in Fig. 7 with the corresponding ones in Fig. 4.

The optimality conditions for an estimate of c_s, however, do become far more stringent when the estimate is made simultaneously with either the sediment density ρ_s, gradient g_s, or thickness h_s. This is consistent with intuition since c_s, ρ_s, g_s and h_s are expected to be statistically coupled since they are physically coupled in a nonlinear way through the bottom reflection coefficient and through a modal or wave number representation of the acoustic field. It is also reasonable that α_s and c_s be statistically uncoupled since the attenuation α_s leads to very slow decay in the field while the sediment sound speed c_s affects coherent modal

propagation and interference that varies far more rapidly over range (this follows because the two parameters appear in separate factors in the modal representation of the waveguide green funciton). It is interesting that thousands of samples are necessary for the variance of c_s to attain the CRLB when the sediment thickness h_s is also an unknown as can be seen by comparing Figs. 5(d) and 7(b) with Figs. 2 and 4. Simultaneous inversion for the sediment layer thickness h_s in these examples tends to induce extremely stringent optimality conditions, such as prohibitively large necessary sample sizes. This implies that sediment thickness and sediment sound speed are highly coupled for the given scenario where sediment thickness equals the acoustic wavelength. This is sensible since as the sediment thickness varies from the wavelength scale in a decreasing manner, for example, the acoustic field will become less sensitive to sediment sound speed. The couplings described in this paragraph are not apparent if only the CRLB is considered, as shown in Fig. 5

The trend of more stringent optimality conditions continues as the number of parameters to be simultaneously estimated is increased. This is shown for the four-parameter simultaneous inversion of c_s, ρ_s, g_s, and α_s in Figs. 8 and 9. The biases, variance terms, and necessary samples sizes are consistently higher than in the cases where the parameters are either inverted alone or with only one other parameter. We find the trend can become less strignent for the estimation of upper sediment layer parameters as the source frequency is increased, but the opposite is typically true for deeper parts of the bottom.

C. Horizontal array versus vertical array

Parameter estimates made from horizontal array measurements are now examined to investigate the effect of array length and orientation on inversion performance. The moments of a c_s estimate from a horizontal array of the same length and center depth as the vertical array of the previous examples are shown in Fig. 10. No improvement is found in the trend but much larger fluctuations appear upon comparing these moments with those for the vertical array in Figs. 2 and 4.

The horizontal array has much poorer angular resolution than the vertical array at the shallow horizontal grazing

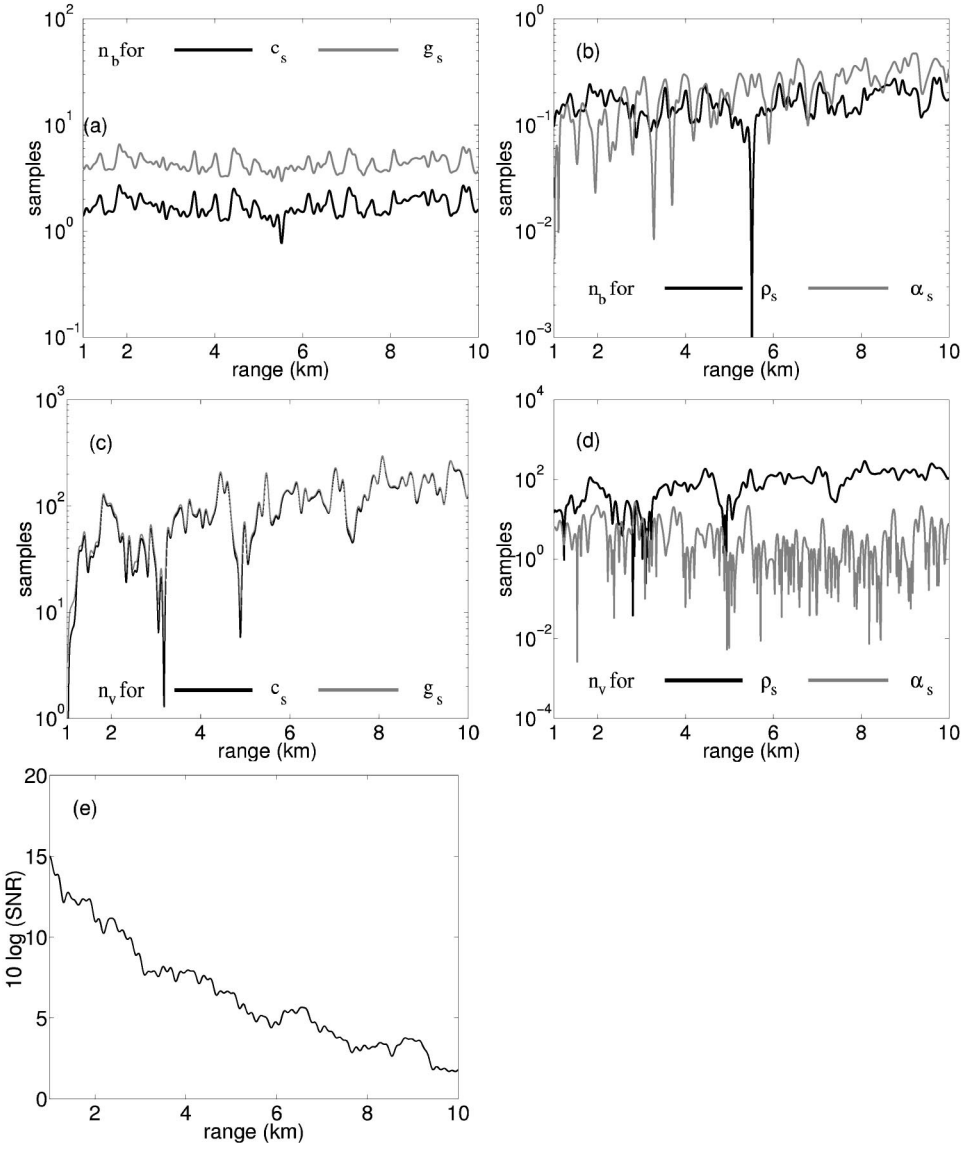

FIG. 12. Simultaneous four-parameter n_b for (a) c_s (black) and g_s (gray), (b) ρ_s (black) and α_s (gray) n_v, (c) c_s (black) and g_s (gray), (d) ρ_s (black) and α_s (gray), and (e) SNR.

angles where the dominant modes typically propagate. This makes it more susceptible to range-dependent fluctuations in SNR arising from the interference of unresolved modes. While the vertical array can resolve the shallow-angle modes with broadside angular resolution of λ/L, the horizontal array receives them at or near end-fire where the angular resolution is only $\sqrt{2\lambda/L}$.

A horizontal array of length $10L$, which can be obtained by synthetic aperture measurements, for example, would be required to have the same angular resolution for shallow grazing angles at 100 Hz as the vertical array of length L. Although this increase in array length greatly reduces the fluctuations in SNR seen in the shorter horizontal array, as shown in Fig. 12(c), it does not provide much improvement in the average trend of the MLE moments. This is illustrated for example in Figs. 11 and 12, where the results for an inversion involving c_s, ρ_s, g_s, and α_s are presented.

Comparing the performance of the long horizontal array in Figs. 11 and 12 with that of the vertical array in Figs. 8 and 9, only the inversion of the bottom attenuation shows some mild improvement. In summary, relatively short vertical arrays can outperform much longer horizontal arrays due to their higher resolving power at shallow grazing angles where dominant modes tend to propagate.

Even if the angular resolution of the receiving array is sufficient to resolve the important modes, further limitations on parameter estimates may emerge depending on the modal content of the field, as discussed previously.

IV. CONCLUSIONS

A reliable method to help attain specified accuracies in the estimation of unknown geoacoustic parameters from remote acoustic measurements is developed to aid the design of geoacoustic experiments. The approach is to compute sample sizes or SNRs necessary for estimates to (1) have variances that asymptotically attain the CRLB and (2) have CRLBs that fall within a specified design error threshold. We show both analytically and with illustrative examples that the former asymptotic condition need not be related to the parameter sensitivity expressed by the CRLB. This is because it involves parameter derivatives of higher order than the CRLB.

Applications to narrow band deterministic signals received with additive noise by vertical and horizontal arrays in typical continental shelf waveguides are explored. For typical low frequency scenarios, necessary SNRs and samples sizes often approach prohibitively large values when a few or more important geoacoustic parameters are unknown, making it difficult to attain practical design thresholds on allowable estimation error. This is found to arise because of the highly nonlinear nature of the geo-acoustic inverse problem and the strong coupling found between many of the important geo-acoustic parameters needed to characterize the acoustic field in an ocean waveguide.

[1] S. D. Rajan, J. F. Lynch, and G. V. Frisk, "Perturbative inversion methods for obtaining bottom geoacoustic parameters in shallow water," J. Acoust. Soc. Am. **82**, 998–1017 (1987).

[2] M. D. Collins, W. A. Kuperman, and H. Schmidt, "Nonlinear inversion for ocean-bottom properties," J. Acoust. Soc. Am. **92**, 2770–2783 (1992).

[3] N. R. Chapman and C. E. Lindsay, "Matched Field inversion for geoacoustic model parameters in shallow water," IEEE J. Ocean. Eng. **21**(4), 347–354 (1996).

[4] S. D. Rajan, "Waveform inversion for the geoacoustic parameters of the ocean bottom," J. Acoust. Soc. Am. **91**, 3228–3241 (1992).

[5] S. E. Dosso, M. L. Yeremey, J. M. Ozard, and N. R. Chapman, "Estimation of ocean-bottom properties by matched field inversions of acoustic field data," IEEE J. Ocean. Eng. **18**(3), 232–239 (1993).

[6] C. E. Linsday and N. R. Chapman, "Matched Field Inversion for geoacoustic model parameters using adaptive simulated annealing," IEEE J. Ocean. Eng. **18**(3), 224–231 (1993).

[7] M. I. Taroudakis and M. G. Markaki, "Bottom geoacoustic inversion by matched field processing- a sensitivity study," Inverse Probl. **16**(8), 1679–1692 (2000).

[8] M. R. Fallat and S. E. Dosso, "Geoacoustic inversions via local, global and hybrid algorithms," J. Acoust. Soc. Am. **105**, 3219–3230 (1999).

[9] D. P. Knobles, R. A. Koch, E. K. Westwood, and T. Udagawa, "The inversion of Ocean Waveguide Parameters using a Non linear least square approach," J. Comput. Acoust. **6**(1&2), 83–97 (1998).

[10] M. I. Taroudakis and M. G. Markaki, "Bottom geoacoustic inversion by broad band Matched Field Processing," J. Comput. Acoust. **6**(1&2), 167–183 (1998).

[11] S. E. Dosso and M. J. Wilmut, "Quantifying data information content in geo acoustic inversions," IEEE J. Ocean. Eng. **27**(2), 296–304 (2002).

[12] H. Schmidt and A. Baggeroer, "Physics-imposed resolution and robustness issues in seismo acoustic parameter inversion," in *Full Field Inversion Methods in Ocean and Seismo-Acoustics*, edited by O. Diaschok *et al.* (Kluwer Academic, Dordrecht, 1995), pp. 85–90.

[13] P. Daly and A. Baggeroer, "Cramer-Rao bounds for shallow water environmental parameter estimation," *OCEANS 97*, MTS IEEE Conference Proceedings (1997), Vol. 1, pp. 430–435.

[14] V. V. Borodin and G. R. Minasian, "Statistical approach to ocean acoustic tomography, Cramer-Rao Lower Bounds for accuracy of sound-speed field reconstruction," in *Full Field Inversion Methods in Ocean and Seismo-Acoustics*, edited by O. Diaschok *et al.* (Kluwer Academic, Dordrecht, 1995), pp. 91–95.

[15] S. E. Dosso and P. L. Nielsen, "Quantifying uncertainty in geoacoustic inversion. II. Application to broadband, shallow water data," J. Acoust. Soc. Am. **111**, 143 (2002).

[16] C. R. Rao, *Linear Statistical Inference and its Applications* (John Wiley & Sons, NY, 1973) p. 326.

[17] E. Naftali and N. C. Makris, "Necessary conditions for a maximum likelihood estimate to become asymptotically unbiased and attain the Cramer-Rao Lower Bound. I. General approach with an application to time-delay and Doppler shift estimation," J. Acoust. Soc. Am. **110**, 1917–1930 (2001).

[18] A. Thode, M. Zanolin, E. Naftali, I. Ingram, P. Ratilal, and N. Makris, "Necessary conditions for a maximum likelihood estimate to become asymptotically unbiased and attain the Cramer-Rao lower bound. II. Range and depth localization of a sound source in an ocean waveguide," J. Acoust. Soc. Am. **112**, 1890–1910 (2002).

[19] M. Betke and N. Makris, "Recognition, Resolution and Complexity of Objects Subject to Affine Transformation," Int. J. Comput. Vis. **44**(1), 5–40 (2001).

[20] S. M. Kay, *Fundamentals of Statistical Signal Processing: Estimation Theory* (Prentice–Hall, Englewood Cliffs, NJ, 1993), p. 19.

[21] D. P. Knobles, R. A. Koch, L. A. Thompson, K. C. Focke, and P. E. Eisman, "Broadband sound propagation in shallow water and geoacoustic inversion," J. Acoust. Soc. Am. **113**, 205–222 (2003).

[22] C. Siedenburg, N. Lehtomaki, J. Arvelo, K. Rao, and H. Schmidt, "Iterative Full Field Inversion Using Simulated Annealing," in *Full Field Inversion Methods in Ocean and Seismo-Acoustics*, edited by O. Diaschok *et al.* (Kluwer Academic, Dordrecht, 1995), pp. 121–126.

[23] S. D. Rajan, J. A. Doutt, and W. M. Carey, "Inversion for the compressional Wave Speed Profile of the Bottom from Synthetic aperture Experiments Conducted in the Hudson Canyon Area," IEEE J. Ocean. Eng. **23**(3), 174–187 (1998).

[24] L. R. Shenton and K. O. Bowman, *Maximum Likelihood Estimation in Small Samples* (Griffin, New York, 1977), p. 7.

[25] N. C. Makris, "The effect of saturated transmission scintillation on ocean acoustic intensity measurements," J. Acoust. Soc. Am. **100**, 769–783 (1996).

[26] N. C. Makris, ''Parameter resolution bounds that depend on sample size,'' J. Acoust. Soc. Am. **99**(5), 2851–2861 (1996).
[27] W. A. Kuperman and F. Ingenito, ''Spatial correlation of surface generated noise in a startified ocean,'' J. Acoust. Soc. Am. **67**, 1988–1996 (1980).
[28] T. W. Anderson, *An Introduction to Multivariate Statistical Analysis* (Wiley, New York, 1971), p. 75.
[29] M. Siderius and P. L. Nielsen, ''Range-dependent seabed characterization by inversion of acoustic data from a towed receiver array,'' J. Acoust. Soc. Am. **112**, 1523–1535 (2002).
[30] P. Ratilal, P. Gerstoft, and J. T. Goh, ''Subspace approach to inversion by genetic algorithms involving multiple frequencies,'' J. Comput. Acoust. **6**(1&2), 99–115 (1998).
[31] S. E. Dosso and P. L. Nielsen, ''Quantifying uncertainty in geoacoustic inversion. II. Application to broadband, shallow water data,'' J. Acoust. Soc. Am. **111**, 143–158 (2002).
[32] I. Ingram, ''Necessary conditions for Geo-Acoustic Parameter Inversions to become Asymptotically Unbiased and Attain the Cramer-Rao Lower Bound,'' Master thesis, Massachusetts Institute of Technology, 2002.